Open Access

Myocardial BOLD Imaging with T2 Relaxation

Nilesh R. Ghugre[1] and Graham A. Wright[*,1,2,3]

[1]*Imaging Research, Sunnybrook Research Institute, Toronto, ON, Canada*

[2]*Department of Medical Biophysics, University of Toronto, Toronto, ON, Canada*

[3]*Schulich Heart Program, Sunnybrook Health Sciences Centre, Toronto, ON, Canada*

Abstract: The purpose of this paper is to present a literature review of the theoretical and experimental work that describes the blood-oxygen-level-dependent or BOLD effect using quantitative T2 relaxation mechanism. The BOLD effect is mediated by paramagnetic deoxyhemoglobin which generates magnetic field inhomogeneities around erythrocytes; T2 is modulated by diffusion of spins in and around erythrocytes. Early work in blood describing the mechanisms of T2 relaxation as a function of oxygen saturation, field strength and cell integrity paved the way towards *in vivo* determination of tissue oxygenation state. Theoretical modeling in blood and tissue microcirculation further shed light into underlying mechanisms of deoxyhemoglobin, leading the way for interrogating myocardial oxygenation state non invasively. From a clinical standpoint, ongoing pre-clinical studies indicate that quantitative T2 may potentially be more specific than signal intensity measures, allowing regional, longitudinal and cross-subject comparison. Furthermore, the T2-based BOLD technique offers greater sensitivity on a 3T scanner, compared to 1.5T, allowing reliable detection of serial changes in perfusion reserve following acute coronary syndrome. We have thus reviewed the theoretical formulations and experimental observations made over several years by many investigators who have given significant insight into the oxygen-sensitive nature of T2 relaxation in blood and hence into the T2-based BOLD effect in tissue microcirculation.

Keywords: Myocardium, Blood, BOLD, T2, Oxygen, Deoxyhemoglobin.

INTRODUCTION

The blood-oxygen-level-dependent (BOLD) effect was initially exploited in functional magnetic resonance imaging (fMRI) studies to probe regional brain activity [1-5]. While oxyhemoglobin is diamagnetic, deoxyhemoglobin is paramagnetic in nature, serving as the endogenous contrast agent in the MRI environment. In other words, blood oxygenation or concentration of deoxyhemoglobin governs the degree of magnetic susceptibility experienced by nearby water protons. The local magnetic field inhomogeneities thus generated cause dephasing of water protons resulting in signal loss, which can be easily sensed by the parameter T2*. Increase in oxygen saturation thus increases T2*-weighted signal while a decrease results in signal loss.

Just as T2*-weighted imaging formed the basis for fMRI brain studies, it was also later applied to assess myocardial blood oxygenation [6-9]. Since myocardial energy metabolism is primarily governed by the balance of oxygen supply and demand, early T2*-based work employed pharmacological vasodilators to perturb myocardial oxygenation in healthy human volunteers [10-12]. At the same time, an analytical description of the BOLD effect in the capillary network of the myocardium was also put forth with T2* as the sensing parameter [13] (later extended to T2 [14]). Since then several investigators have applied T2*-based myocardial BOLD imaging in the clinical setting to evaluate patients with cardiovascular complications viz. hypertensive hypertrophy, stress-induced angina/ischemia, impaired left ventricular contraction, coronary artery stenosis [15-19].

In contrast to the T2* approach, others simultaneously investigated the BOLD effect using the MRI transverse relaxation time, T2. The first study to characterize the effect of field strength and blood oxygenation on T2 relaxation time was by Thulborn *et al*. [20]; this work showed that increase in $T2^{-1}$ with deoxyhemoglobin concentration arose from diffusion of protons through the generated magnetic field disturbances. Following this, several *in vitro* studies sought to systematically characterize the effects of whole blood oxygen saturation on T2 relaxation [21-23]; the *in vivo* application was later demonstrated [24, 25] suggesting its potential clinical utility. After the *in vitro* validation in blood, the quantitative T2-based BOLD technique was finally applied towards assessing *in vivo* myocardial oxygenation state by several investigators [26-30]. Similar to T2* studies, the authors perturbed the balance between myocardial oxygen demand and supply through vasodilatory agents allowing estimation of clinically-relevant parameters like perfusion reserve and oxygen extraction fraction. Besides T2 quantification, others have also evaluated signal intensity-based approaches to identify regional differences in myocardial blood flow using T2-weighted imaging [31-33]. Along with myocardial applications, effects of blood oxygenation within skeletal muscle microcirculation have also been investigated using transverse relaxation time [34,35].

*Address correspondence to this author at the Sunnybrook Health Sciences Centre, 2075 Bayview Ave., Rm. S6 65, Toronto, ON, M4N 3M5, Canada; Tel: (416) 480-6869; Fax: (416) 480-5714;
E-mail: graham.wright@sri.utoronto.ca

1874-3471/12 2012 Bentham Open

More recently, steady-state free precession (SSFP) imaging has also been explored to assess regional myocardial oxygenation in a canine model of coronary artery stenosis [36,37]. This was based on prior theoretical and experimental work in blood by Dharmakumar and colleagues [38], which employed the Luz-Meiboom two-compartment model [39] consisting of plasma and red blood cells. It was demonstrated that oxygen-contrast in SSFP methods arose from diffusion of spins through magnetic inhomogeneities generated by deoxygenated erythrocytes, rather than sensitivity from bulk off-resonance frequency fluctuations. Similar validations were also performed in muscle microcirculation using a model of intra- and extravascular pools [40]; this was later extended to healthy human volunteers using an ischemic leg cuff model [41]. Other groups have similarly demonstrated the utility of steady-state techniques to detect BOLD changes in both brain and muscle using a visual activation task and ischemia/ hyperemia model respectively [42,43].

The purpose of this paper is to present a literature review of the theoretical and experimental work that describes the BOLD effect using quantitative T2 relaxation mechanism. The review is organized in the following manner. The first section gives a quick overview of the properties of blood. The second section describes the relaxation mechanisms in blood with regard to the oxygen state and form of hemoglobin. The third section describes the initial studies that demonstrated the oxygen dependence of T2 in both *in vitro* and *in vivo* settings. The fourth section briefly talks about validation of the oxygen-sensitive effect of T2 within muscle microcirculation. This leads into the fifth section describing the application of the BOLD theory to myocardial tissue, thereby allowing estimation of several clinically relevant parameters. The future directions and clinical relevance of the T2-based myocardial BOLD effect are discussed in the sixth section. This section describes the importance of moving to higher field strength (3T) and stresses on the ability of the T2 approach to perform regional, longitudinal as well as cross-subject comparison/ evaluation of a given disease state in a very systematic and quantitative manner. The ongoing work in our group's laboratory, using the T2-based BOLD approach in the myocardium has also been mentioned along with potential clinical applications. The conclusions are drawn at the end of the review.

PROPERTIES OF BLOOD

Blood primarily comprises of 55% plasma and 44% erythrocytes (red blood cells) with the remaining 1% formed by leukocytes (white blood cells) and thrombocytes (platelets). The water molecules (protons) in plasma that are detectable by MRI are in the form of bulk water, which constitutes about 90% of blood by volume. Erythrocytes carry the oxygen-transport protein, hemoglobin (Hb), which is the predominant macromolecule in blood. The heme iron, in the ferrous Fe^{2+} state, present in hemoglobin gives it its oxygen-carrying capacity and also its magnetic properties.

When blood exits the pulmonary circulation, hemoglobin forms oxy-hemoglobin (oxyHb) in the oxygen-rich environment of the lungs. The arterial supply from the heart then carries the oxygenated blood to different tissues where oxygen is taken up by the cells to maintain energy, metabolism and function. Once oxygen is extracted in the tissue microcirculation, hemoglobin is converted to deoxyhemoglobin (deoxyHb) as blood is returned to the heart via venous supply. Thus hemoglobin switches between oxyHb and deoxyHb as blood moves through the circulation; arterial blood contains approximately 5% deoxyHb while venous blood contains 30%. If blood is removed from the circulation (e.g. hemorrhage), hemoglobin undergoes oxidative denaturation to form methomoglobin (metHb), which contains iron in the ferric Fe^{3+} state.

The magnetic properties of hemoglobin and its forms have been described in detail [44-46]. Hemoglobin in the oxygenated form is diamagnetic in nature since it does not possess any unpaired electrons. On the other hand, deoxyHb and metHb have 4 and 5 unpaired electrons respectively, giving them paramagnetic properties. Consequently, MRI relaxation times of blood are modulated by the structure of Hb and its oxidation state. This review primarily focuses on the T2 relaxation properties of blood that are a function of the paramagnetic nature of deoxyHb; effects of metHb are beyond the scope of this paper.

RELAXATION IN BLOOD

MR imaging typically involves a 90° radio frequency (rf) excitation pulse, applied at the Larmor frequency, that rotates the proton magnetic moments into the transverse plane relative to the direction of the applied magnetic field (or B_0). Once in the transverse plane, the loss of phase coherence among the spins in termed as transverse relaxation and the time taken for the transverse magnetization to reach 1/e of its equilibrium value is defined as T2 relaxation time. The difference in phase among the precessing spins occurs as a result of them experiencing different local magnetic fields in time. In blood, the T2 relaxation mechanism can be explained with two effects, diamagnetic and paramagnetic relaxation.

Since oxyHb is diamagnetic, T2 of fully oxygenated blood is dominated by diamagnetic or spin-spin relaxation effects, which include rotational Brownian motion of both water molecules and macromolecule hemoglobin along with their interaction with one another. Starting with the T2 expression from Bloembergen's theory of nuclear magnetic relaxation [47], relaxation in hemoglobin solutions can be written in a simplified form as follows,

$$\left(\frac{1}{T2}\right) = F_P \cdot A \cdot \tau_r \cdot \left(0.3 + \frac{0.7}{1+\left(f_0 / 0.8 f_r\right)}\right) \quad (1)$$

where, F_p is the fraction of time spent by the water proton attached to hemoglobin thereby sharing its motion. $A=1.5\ \gamma^4 h^2 r^{-6}=5.4\text{x}10^{10}\ s^{-1}$ is a single representation of various constants, where γ is proton gyromagnetic ratio, h is Planck's constant and r is the proton-proton distance. τ_r is the correlation time i.e. the time required for the rotational Brownian motion to produce an appreciable change with respect to B_0. f_0 is the Larmor frequency and $f_r=(2\pi\tau_r)^{-1}$ is the cut-off frequency.

As a first approximation, relaxation in blood with only oxyHb can be considered to be similar to that in hemoglobin solutions. However, *in vivo* blood cycles between oxy and deoxy state as it is circulated in the system. In this case, the paramagnetic relaxation effects of deoxyHb (in erythrocytes) become an important mechanism affecting the transverse relaxation time. The magnetic inhomogeneities thus generated create a susceptibility difference between plasma and erythrocytes, resulting in differences in precession frequency of spins present in or around these pools. In T2-weighted imaging sequences, the 180° refocusing pulses applied to the transverse magnetization can restore the lost phase coherence among the spins by reversing their accumulated phase differences. However, if diffusion effects dominate relative to the refocusing interval then this results in an additional signal loss, which cannot be corrected by the 180° pulses. In contrast if the imaging sequence uses gradient echos for refocusing spins, then this becomes sensitive only to magnetic susceptibility (or phase) differences generated by paramagnetic deoxyHb. The T2* approach is based on this mechanism, however the details are not discussed in this review.

Thus the primary mechanism for oxygen-sensitivity of T2 in blood can be attributed to random motion of water molecules in and around the magnetic field fluctuations present in the erythrocyte vicinity. If plasma and erythrocytes can be considered as two compartments or sites is the blood system, then proton exchange between the two compartments can be analogous to the theory of two-site chemical exchange mechanism reviewed and formulated by Allerhand and Gutowsky [48]. According to the two-site model, the diffusion- or exchange-sensitive relaxation rate $(1/T2)_D$ can be expressed with the following equation [39],

$$\left(\frac{1}{T2}\right)_D = 4\pi^2 F_a F_b \tau_e \left(\Delta f\right)^2 \left[1-\left(2\tau_e / TE\right)\tanh\left(TE/2\tau_e\right)\right] \quad (2)$$

where, Fa and Fb represent the fraction of protons in the two sites, Δf is the Larmor precession frequency difference between the two sites and TE is the echo time. τ_e is the exchange time between the two sites and can be represented by the equation, $\tau_e^{-1} = \tau_a^{-1} + \tau_b^{-1}$, where τ_a and τ_b are the residence times of protons at the respective sites. The work of Thulborn *et al.,* [20] (discussed in the next section) provided experimental evidence for the role of diffusion-based paramagnetic effect in modulating T2 relaxation in whole blood. For a more comprehensive review of the relaxation mechanisms in stationary blood, the article by Brooks and Di Chiro provides an excellent reference [49].

OXYGEN DEPENDENCE OF T2 IN BLOOD

In Vitro

The oxygen dependence of T2 relaxation in whole blood was first demonstrated by Thulborn *et al.,* over a range of Larmor frequencies between 80 and 469 MHz (1.9 and 11 T) [20]. Transverse relaxation rate enhancement $T2^{-1}_{ex}$ ($T2^{-1}_{(venous)} - T2^{-1}_{(arterial)}$) was shown to be quadratically related to field strength while $T2^{-1}$ was similarly related to the fraction of deoxyHb present in blood. The study also found that volume magnetic susceptibility of erythrocytes increased with deoxygenation thereby generating strong magnetic gradients around the cells. This result coupled with the dependence of $T2^{-1}_{ex}$ on the interecho spacing of the Carr-Purcell-Meiboom-Gill experiment led to the conclusion that transverse relaxation rates in blood are governed by dephasing of water molecules via diffusion through field gradients, that are a function of deoxyHb fraction.

While the work of Thulborn *et al.,* concentrated on the medium and high field relaxation behavior in blood, Gomori *et al.,* [21] explored the mechanisms in the low or (at the time) clinically-relevant field strength. They demonstrated similar T2 relaxation dependence on field strength (0.19-1.4T) and interecho spacing for oxyHb, deoxyHb and metHb in intact red blood cells; metHb produced 1.6 times stronger relaxation enhancement compared to deoxyHb. Lysed red blood cells produced T2's that were independent of field strength and interecho spacing due to the magnetically homogeneous environment that they create. Comparing their low field data with the high field observations by Thulborn *et al.,* it was concluded that difference in T2 at the two field extremes arose from reduced diffusion sensitivity at low magnetic fields.

Both Thulborn *et al.,* and Gomori *et al.,* represented the T2 relaxation in blood in accordance with a modified multi-site chemical exchange theory of Luz and Meiboom; the transverse relaxation can then be put in the form,

$$\frac{1}{T2} = \delta^2\left[1-\frac{\tau_D}{2\tau_{CPMG}}\tanh\left(\frac{2\tau_{CPMG}}{\tau_D}\right)\right]\tau_D\sum_i \rho_i\left(\Delta H_i\right)^2 \quad (3)$$

where, δ is the gyromagnetic ratio of proton, τ_D is the correlation or exchange time, ΔH_i represents the difference between the field strength in the i^{th} region and the average field strength, p_i is the probability that a proton is present in the i^{th} region and τ_{CPMG} is the interecho spacing. For a given field strength, the interecho spacing dependence of T2 as observed from *in vitro* experiments was fit to the above equation and estimates of correlation times were obtained.

In Vivo

Apart from the quantitative *in vitro* study by Thulborn *et al.,* relating T2 to percent oxygenated hemoglobin ($\%HbO_2$), early *in vivo* work was only qualitative [4,50,51] in nature. In this respect, Wright *et al.,* [23] derived an *in vivo* calibration between T2 and oxygen saturation and hence non invasively estimated $\%HbO_2$ of vascular blood on a 1.5T clinical scanner. First, an *in vitro* calibration relating T2 and $\%HbO_2$ was derived for human blood and characterized by the Luz-Meiboom two-site exchange model [39]. Second, *in vivo* T2 measurements were made in blood vessels of the mediastinum of healthy subjects. Finally, *in vivo* $\%HbO_2$ was computed from corresponding T2 measurements using *in vitro* calibrations as a reference.

Similar to eqn. 3, the effect of hemoglobin oxygenation on T2 of blood can be described by a modified form of the two-site proton exchange model of Luz-Meiboom [39], given by,

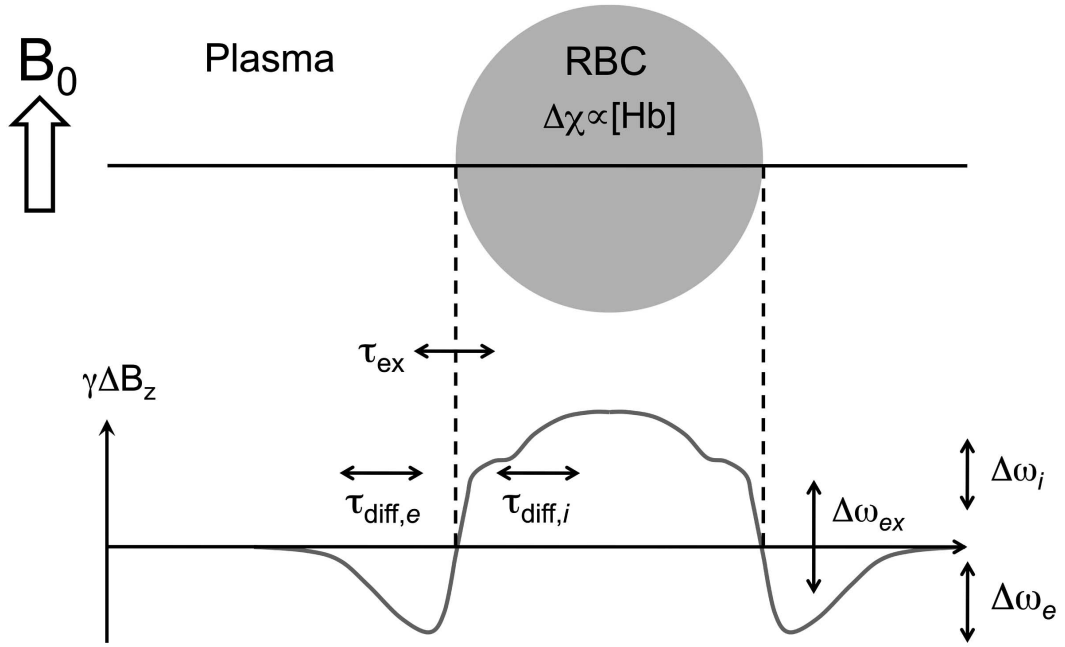

Fig. (1). The schematic shows the relevant parameters involved when protons interact with a red blood cell (RBC) within blood plasma in the presence of an external magnetic field B_0. The magnetic susceptibility of the erythrocyte increases in proportion with the concentration of deoxyhemoglobin in blood and $\gamma\Delta B_z$ is the corresponding frequency shift produced. τ_{ex} is the correlation time for proton exchange and $\Delta\omega_{ex}$ is the corresponding frequency shift. $\Delta\omega_i$ and $\Delta\omega_e$ represent the change in precession frequency in the intracellular and extracellular pools as a result of proton diffusion in these pools.

$$\frac{1}{T2_b} = \frac{1}{T2_0} + (P_A)(1-P_A)\tau_{ex}\left[\left(1-\frac{\%HbO_2}{100\%}\right)\alpha\omega_0\right]^2 \times \left(1-\frac{2\tau_{ex}}{\tau_{180}}\tanh\frac{\tau_{180}}{2\tau_{ex}}\right) \quad (4)$$

where, $T2_b$ is the transverse relaxation time of fully oxygenated blood, P_A is the fraction of protons present at one site, τ_{ex} represents the exchange time i.e. time taken by a proton to move between the two sites, α is a dimensionless measure of the susceptibility of deoxyhemoglobin and erythrocyte geometry, ω_0 is the proton resonant frequency and τ_{180} is the interecho spacing or interval between 180° refocusing pulses. One of the sites can be considered as that under the influence of gradient fields generated by erythrocytes with the frequency difference between the two sites represented by the squared term (containing $\%HBO_2$) in the above equation. The equation suggests that the strength of the oxygen effect increases quadratically with field strength while sensitivity of $T2_b$ to $\%HbO_2$ increases with τ_{ex}. Fig. (**1**) shows a schematic of the interaction of protons at the two sites viz. red blood cell and plasma along with relevant parameters.

Since the primary intent was to calibrate T2 for changes in $\%HbO_2$ and not probe underlying effects of other parameters, α, τ_{ex} and P_A [21,52-54], the above equation was compacted to the form,

$$\frac{1}{T2_b} = \frac{1}{T2_0} + K(\tau_{180},\omega_0)\left(1-\frac{\%HbO_2}{100\%}\right)^2 \quad (5)$$

where, K represents the lumped parameter for a given biological system and is a function of the experimental parameters, interecho spacing and field strength. Based on this form, oxygen effect is governed by 1) $T2_0$, which depends on temperature and hematocrit [55] and 2) K, which increases with ω_0 and τ_{180}.

The pulse sequence used for the *in vivo* estimation of $T2_b$ consisted of an inversion pulse for fat suppression followed by a frequency-selective 90° pulse for exciting water protons. The transverse magnetization was then refocused every τ_{180} ms by 180° rectangular pulses played out in an MLEV pattern [56] which constitutes the T2 preparation period. The signal was finally sampled using a spiral readout. Imaging was performed on a 1.5T GE system.

The *in vitro* calibration of $T2_b$ involved venous blood draws, from volunteers, which were aerated over a range of $\%HbO_2$ (30-96 %). T2 values were measured for τ_{180} = 6, 12, 24 and 48 ms with TR=2s and TEs from 24-384 ms; a monoexponential signal decay model was used. Fig. (**2**) shows images of blood samples drawn from a representative volunteer at different echo times and varying levels of oxygenation.

For each τ_{180}, the $T2_b$ *vs*. $\%HbO_2$ data points were fitted by eqn. 5 using a least-squares algorithm and corresponding K and $T2_0$ values were estimated. Eqn. 5 was a reasonable representation of the data; Fig. (**3**) demonstrates the effect of interecho spacing on the $T2_b$-HbO_2 calibration by plugging in the estimated parameters. When τ_{180} was increased from 6 ms to 48 ms, K increased from 13 s^{-1} to 62 s^{-1} while $T2_0$ decreased in a less dramatic way (260 to 236 ms). The results indicated that larger values of K represented greater $\%HbO_2$ effect and that $T2_0$ was relatively less sensitive.

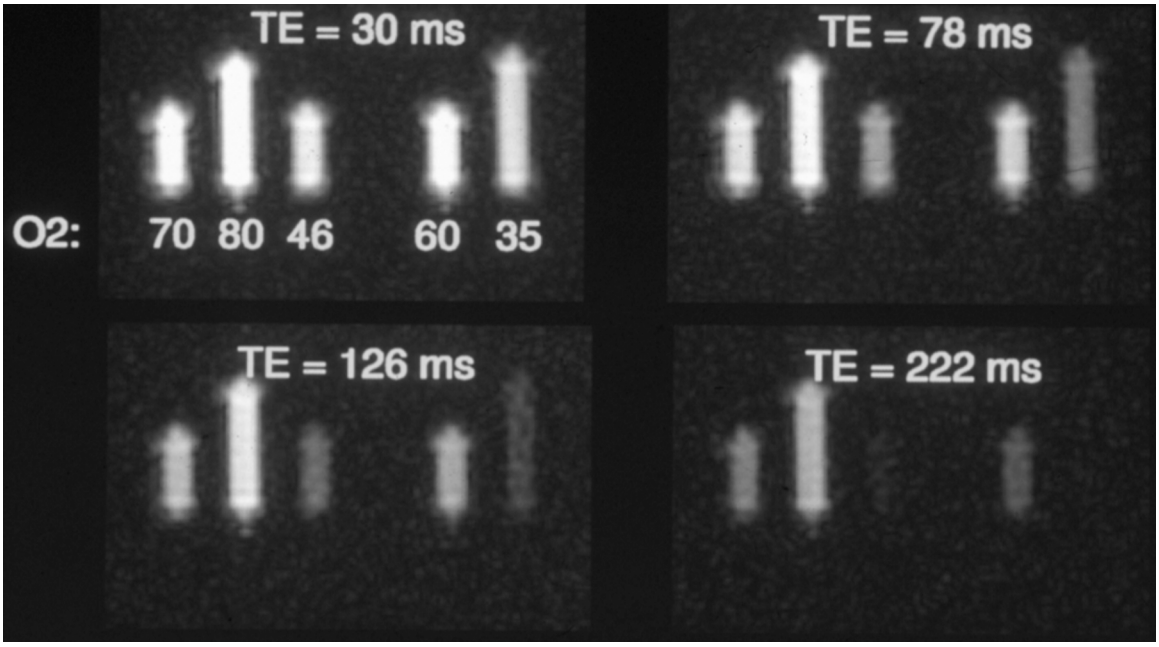

Fig. (2). Images demonstrate the T2-weighted signal loss within blood samples as a function of echo time. The vial's contained blood drawn from a representative volunteer and manipulated to give varying levels of oxygenation.

The *in vivo* study involved calculating $T2_b$ values in the aorta, superior vena cava and pulmonary trunk of healthy volunteers. Average T2's from venous blood (superior vena cava) were shorter than arterial blood (aorta) as expected (145 vs. 222 ms) and were within the range of *in vitro* observations. $T2_0$ was calculated assuming a $\%HbO_2$ of 97% for aortic blood for minimum τ_{180}, $\%HbO_2$ was then estimated using eqn. 5. The estimate of oxygen saturation in venous blood (range of 72-78%) was in accordance to that mentioned in literature.

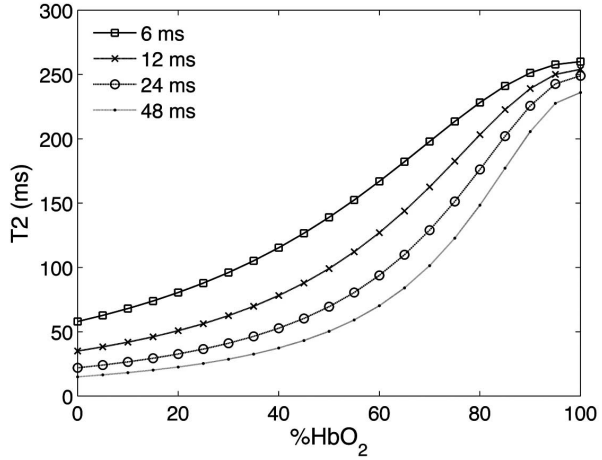

Fig. (3). Plot demonstrates the relationship between $T2_b$ and $\%HbO_2$ for τ_{180} varying from 6 ms to 12 ms. The curves were computed from eqn. 5 using appropriate values of K and $T2_0$.

Encouraged by the ability to quantify the oxygen state of blood *in vivo*, Foltz *et al.,* [24] went ahead to quantify coronary venous oxygen content specifically in conjunction with coronary flow reserve using T2 quantification. In the case of ischemic heart disease there is need to carefully monitor coronary blood oxygen supply with respect to demand state of myocardium. Coronary flow reserve is reduced in patients with coronary artery disease and is restored after therapeutic intervention [57,58]. The authors wanted to explore the utility of MRI-based non-invasive oxygen sensitive technique to assess myocardial supply and demand characteristics in a quantitative manner. Blood oxygen supply and demand was modeled using Fick law, which states that blood flow (Q) within a tissue system increases in proportion to rate of oxygen consumption and is inversely related to arteriovenous (art, ven) difference in blood oxygen content; this can be represented in the form,

$$Q(L/\min/g) = \frac{Cardiac\ metabolic\ rate\ of\ O_2\ (ml/\min/g)}{\left(\left(\%O_{2,art} - \%O_{2,ven}\right) * [Hb]\right)(ml/L)} \tag{6}$$

where, [Hb] is the hemoglobin concentration. In other words, oxygen supply is represented by flow Q and demand by metabolic/consumption rate of O_2; either of these two independent parameters can be estimated with knowledge of arterial and venous oxygen content. A pharmacological vasodilator, Dipyridamole, was used to uncouple supply and demand. Dipyridamole is an arteriolar vasodilator which does not induce any significant increase in myocardial energy demand [59]. This implies that vasodilatory-induced changes in blood oxygenation would be a direct reflectance of changes in coronary blood flow. The study assumed that oxygen supply and demand was successfully uncoupled and that arterial oxygen content was unchanged during vasodilation, then coronary flow reserve could be computed using eqn. 6 as follows,

$$CFR = \frac{Q_{peak}}{Q_{basal}} = \frac{\left(\%O_{2,art} - \%O_{2,ven,basal}\right)}{\left(\%O_{2,art} - \%O_{2,ven,peak}\right)} \tag{7}$$

where, basal and peak correspond to rest and vasodilatory states and $\%O_{2,\,art}$ was assumed to be 97%. T2 values were measured in the coronary sinus (representing $\%O_{2,\,ven}$) of

five healthy volunteers using a T2-prepared spiral imaging sequence similar that described by Wright *et al.* [23]. The T2 values, in both rest and vasodilatory state, were then mapped to blood oxygenation level using *in vitro* $T2_b$-$\%HbO_2$ calibration similar to Wright *et al.* [23]. Finally, using eqn. 7, an average coronary flow reserve was found to be 1.8. An underestimation of CFR, compared to a value of 4 from previous studies [60], was attributed to 1) right atrial mixing, 2) insufficient supply-demand uncoupling by Dipyridamole; literature suggests that cardiac metabolic rate increases by ~30% [59] and 3) heterogeneity and temporal changes in Dipyridamole action. Nevertheless, the study successfully demonstrated the clinical utility of noninvasively estimating coronary oxygenation by T2-based quantification. In a similar manner, several other studies have also utilized the oxygen saturation effect in MRI in preclinical models as well as in a clinical setting [61-65].

Following this study of Foltz *et al.* [24], Yang *et al.,* [25] recently extended the MRI-based oximetry approach to determine oxygen consumption in the myocardium (MVO_2) and whole body (VO_2) in a non-invasive manner. The basis of the study was that MVO_2, which represents overall myocardial oxidative metabolism, might be a better indicator of predicting LV dysfunction and heart failure compared to left ventricular (LV) ejection fraction [66]. Furthermore, VO_2 has been shown to have prognostic value in assessing patients with coronary heart disease and heart failure [67,68]. The study was conducted in 13 healthy human volunteers in each of whom *in vitro* blood T2-$\%O_2$ calibration was derived [23] by drawing venous blood samples and subsequently varying oxygen saturation. T2 measurements were performed in coronary sinus (CS) and main pulmonary artery (MPA) using T2-prepared spiral imaging sequence [24]; CS and MPA oxygenation was then computed using the T2-%O2 calibration curve. Finally, MVO_2 and VO_2 were obtained from CS and MPA oxygenation respectively using Fick's law. CS and MPA flow measurements were performed using phase contrast gradient echo sequence and LV mass was calculated using 2D FIESTA sequence. The average MVO_2 was 11 ml/min per 100g LV mass while VO_2 was 3.8 ml/min/kg body weight, these values were in good agreement with those previously published [68,69]. Current techniques for measuring MVO_2 and VO_2 are either indirect or invasive. Moreover, non-invasive PET approach which is considered the gold standard, is limited by low-availability, high expense and (importantly) the use of radioactive tracers. In comparison, MRI-based BOLD approach offers a promising alternative to estimate myocardial and whole-body oxygen consumption.

Effect at 3T

After the derivation of the $T2_b$-$\%HbO_2$ calibration curve at 1.5T and demonstrating its utility in the *in vivo* estimation of oxygen saturation [23], Lee *et al.,* interrogated the dependence of MR relaxation parameters on blood oxygenation at 3T. The authors considered eqn. 5 as the starting point for relaxation in blood where the parameter K is a function of echo spacing τ_{180} and is expected to have a quadratic dependence on field strength for a given system. Venous blood drawn from human healthy volunteers was manipulated by nitrogen gas or air to obtain varying levels of oxygen saturation (40-90%). *In vitro* blood calibrations of $T2_b$-$\%HbO_2$ thus obtained, demonstrated that K increased from 1.5T to 3T by a factor of 3.4 and this increase was independent of τ_{180}. The drop in $T2_0$ at 3T (239 *vs*. 165 ms) was consistent with the findings of Thulborn *et al.* [20]. Fig. (**4**) demonstrates the effect of field strength on the $T2_b$-$\%HbO_2$ relationship for τ_{180} = 12 ms; plot was obtained by plugging values of K and $T2_0$ in eqn. 5. Using the *in vitro* calibration, the femoral vein oxygenation in the volunteers was found to be ~70% at both 1.5T and 3T, consistent with literature values. It was also shown that *in vivo* scans of the thigh produced greater SNR at 3T than 1.5T (a factor of 1.35). Overall, the study demonstrated the feasibility of using a 3T clinical system for *in vivo* oximetry and the observations suggest that T2-based BOLD effect would be greater at 3T in comparison to 1.5T.

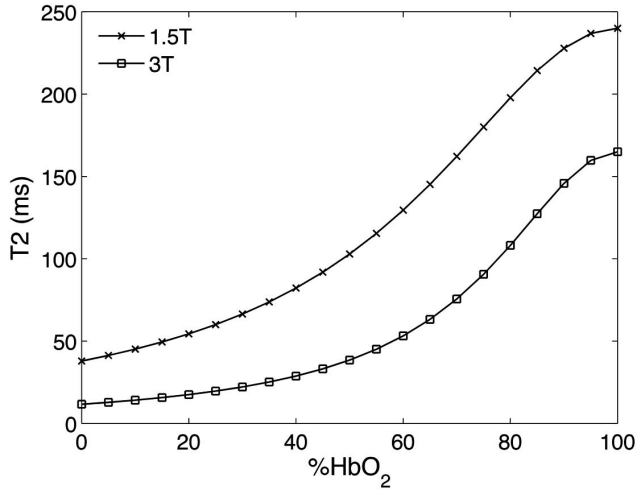

Fig. (4). Plot demonstrates the $T2_b$-$\%HbO_2$ calibration curves for 1.5T (K=28.3, $T2_0$=225.8 ms) and 3T (K=100, $T2_0$=175.7 ms) as obtained from eqn. 5 for τ_{180} = 12 ms.

BOLD EFFECT IN SKELETAL MUSCLE

BOLD effect has been shown to arise from diffusion of water protons through magnetic field fluctuations generated by paramagnetic deoxyHb present in blood. Early studies have mainly concentrated on describing oxygenation effects in blood, however, expansion of this work to tissue microcirculation is clinically valuable in order to assess tissue viability and function [70-74]. In order to probe blood oxygenation levels in a given tissue system, it is necessary to consider a multi-compartment model, unlike a monoexponential signal decay model employed for characterizing effects in blood. Multi-exponential signal decay has been previously demonstrated in normal muscle identifying two or three T2 components [75-79]. If a two compartment model is considered, then according to Le Rumeur [79], the long and short T2 components represent vascular space and a combination of (intracellular and interstitial) space respectively.

Based on this observation, Stainsby and Wright [35] went ahead to explore the possibility of using the long T2 component to indicate the oxygen state of blood within tissue microcirculation. *In vivo* T2 measurements were performed in rabbit skeletal muscle and a biexponential signal decay model was used to describe MRI signal behavior. A two-site

proton exchange model was considered [78,80,81] with the following set of equations describing the model,

(a) $s(t) = P_S \cdot e^{-t/T2_S} + P_L \cdot e^{-t/T2_L}$

(b) $T2_S = \frac{1}{c_1 + c_2}$

(c) $T2_L = \frac{1}{c_1 - c_2}$

(d) $P_S = \frac{1}{2} - \frac{1}{4c_2} \cdot \left(\left(f_E - f_I\right) \cdot \left(\frac{1}{T2_I} - \frac{1}{T2_E} \right) + k_E + k_I \right)$ (8)

(e) $P_L = 1 - P_S$

(f) $c_1 = 0.5 \cdot \left(\frac{1}{T2_I} + k_I + \frac{1}{T2_E} + k_E \right)$

(g) $c_2 = 0.5 \cdot \sqrt{\left(\frac{1}{T2_E} - \frac{1}{T2_I} + k_E - k_I \right)^2 + 4 \cdot k_I \cdot k_E}$

where, $T2_S$ and $T2_L$ are the short and long T2 components observed with P_S and P_L being the relative weights respectively. The indices *I* and *E* represent the intra- and extravascular pools respectively with 1) f denoting relative volume fraction of the two pools (f_I, f_E=1-f_I), 2) k representing proton exchange rate from one pool to the other (k_I, k_E) with the relation, ($k_E.f_E$)/f_I = -k_I = K and 3) $T2_I$ and $T2_E$ being the corresponding relaxation times in blood (dependent on oxygen state) and tissue (fixed) respectively. For skeletal muscle, it was assumed that K=4 Hz [80], $T2_E$ = 27 ms and f_I = 3%. Theoretical predications indicate that $T2_L$ is sensitive to changes in oxygenation but not $T2_S$.

Rabbits were imaged on a 1.5T GE system with T2 measurements performed using a multi-echo imaging sequence consisting of a train of refocusing pulses (8 ms interval) in an MLEV pattern. Blood oxygenation state in each animal was altered by delivery of variable mixtures of oxygen and nitrogen through a breathing mask. No correlation (r=0.17) was found between monoexponential T2 values and blood oxygen state; this was attributed to the relatively low blood volume fraction of 3% in muscle making the model insensitive. On the other hand, the long T2 component ($T2_L$) of the biexponential fit was significantly correlated with $\%O_2$ (r=0.62) with the short T2 component ($T2_S$) relatively unchanged (26 ms). The trend of experimental results ($T2_L$ *vs*. $T2_{blood}$) was similar to theoretical predictions. The authors also discuss computing actual T2 of blood in the tissue ($T2_I$) in terms of $T2_L$, thereby allowing estimation of the actual oxygen state in the microcirculation; this $T2_I$ value can then be plugged into the *in vitro* $T2_b$-$\%HbO_2$ calibration curve derived by Wright *et al.* [23].

In a parallel study, Noseworthy *et al.,* [34] demonstrated the utility of the bi-component T2 model to track oxygen effects in skeletal muscle of healthy human volunteers under normoxic (air, 20.8% O_2) and hyperoxic (100% O_2) conditions. Similar to the work of Stainsby *et al.*, it was observed that the short T2 component ($T2_S$), reflecting extravascular (cellular + interstitial) space, was unchanged with oxygen state while the long component ($T2_L$), representing blood, was oxygen sensitive. $T2_L$ increased with hyperoxia with the effect more prominent in slow twitch (soleus) muscle compared to fast twitch (gastrocnemius). Clinically, this finding would be very useful to estimate degree of tissue hypoxia in cases of vascular disease.

BOLD EFFECT IN MYOCARDIUM

Several early studies employed signal intensity-based techniques to demonstrate the correlation between myocardial signal and blood oxygenation state [6,8,9]. However, the first study to relate hemoglobin saturation with T2 relaxation in myocardium was performed by Atalay *et al.* [26]; this was hence quantitative in nature rather than qualitative. The study was carried out on a 4.7T GE NMR spectrometer in which isolated rabbit hearts, arranged in Langendorff mode, were imaged. A line scan protocol using Hahn spin echo was employed to measure T2 with the echo time TE varying between 18 ms and 1 s. T2 values were computed in the myocardium for varying levels of hemoglobin saturation, that could be controlled by changing the partial pressure of oxygen in the perfusate.

T2 measurements in both septum and left ventricular free wall were found to increase with hemoglobin saturation. Septal T2 was quadratically related to %Hb, very similar to behavior in blood although less pronounced; reasons for this would be the relatively less blood volume within the myocardium along with modified susceptibility gradients at the tissue-vessel interface. The authors also comment on the difference between relaxation rates R2 (1/T2) and R2* (1/T2*) with respect to %Hb sensitivity, suggesting that sensitivity of R2* is slightly greater that R2 due to a steeper curve.

After their initial study looking at $\%O_2$ changes in coronary sinus of humans [24], Foltz *et al.,* [27] later extended their work to the myocardium by observing vasodilator response with T2 relaxation. Since vasodilation-induced signal changes may reflect changes in either blood volume (BV) or $\%O_2$ within the microvasculature, the study sought to characterize their relative contributions to T2 changes. An intracoronary infusion of adenosine was used in the study, which would increase only perfusion and leave BV or cardiac metabolic rate/O_2 consumption unaffected. Under these conditions, it was hypothesized that changes in T2 would reflect changes in oxygen levels in the microcirculation.

T2 quantification was performed using a previously validated T2-prepared spiral imaging sequence [24]. Blood volume assessment was done using T1 quantification in myocardium and blood, before and after injection of an intravascular contrast agent (Clariscan) based on a model described by Bauer *et al.* [82]. Oxygen levels were estimated via blood drawn from the left anterior descending (LAD) coronary vein while perfusion was computed using a Doppler flow wire placed in the left main coronary artery. Myocardial T2 was elevated by 17% with vasodilation and was associated with a coronary perfusion reserve of 3.2 and a 56% change in coronary venous oxygenation. Both blood volume and cardiac metabolic rate (heart rate x blood pressure) were unchanged with adenosine.

Identifying perfusion deficit is clinically important to differentiate between viable and injured myocardium (at-risk or infarcted); sensitivity to a 2-fold reduction in perfusion reserve is essential [83]. Fig. (**5**) shows the relationship between change in microcirculation oxygen levels and perfusion reserve as predicted by Fick's law, eqn. 6 [24]. A perfusion reserve of 3-fold observed in this study maps to a microcirculation $\Delta\%O_2$ of 40%. In comparison, a T2 elevation of 10% is required for detecting a 40% change in oxygen levels based on the two-pool model [35]. Hence the study concludes that a vasodilatory change in T2 can detect about a 40% change in microcirculation oxygen levels. The authors comment that although this appears to be less that the required diagnostic sensitivity, it should be sufficient to distinguish normal from abnormal myocardium.

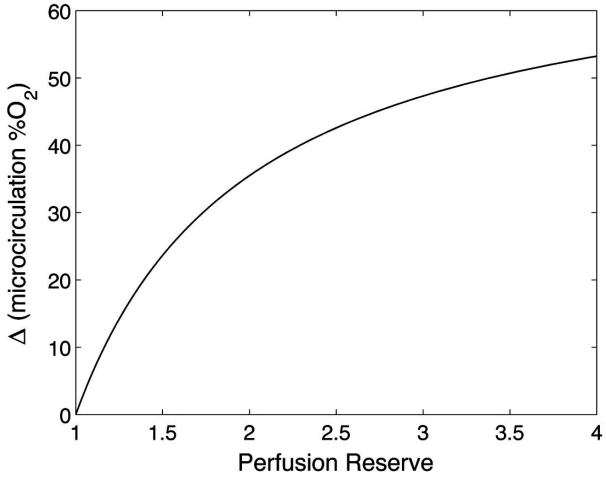

Fig. (5). The curve shows the relationship between changes in microcirculation oxygenation and perfusion reserve as predicted by Fick's law.

Vasodilatory-change in myocardial T2 was also exploited by Zheng and colleagues to probe the coupling between myocardial oxygen supply and demand, which is an important consideration in coronary artery disease. The oxygen supply-demand balance was represented by the term oxygen extraction fraction (OEF) that is defined by the ratio ($O_{2,\ artery} - O_{2,\ vein}$)/($O_{2,\ artery}$). In their initial work, they derived the theoretical relationship between T2 and OEF and validated the relaxation effects using both computer simulations and experimental work in canines [29,30]. Vasodilation was induced by dipyridamole to perturb the supply-demand characteristics. Myocardial T2 was shown to increase by 16% (44 ms *vs*. 51 ms) from rest to peak dipyridamole effect. OEF measured by MRI demonstrated a strong correla-tion with that measured from blood sampling (R=0.83). A two-compartment model consisting of intra- and extravas-cular magnetizations was proposed by the authors to relate the various parameters of the myocardial tissue system viz. T2, OEF, myocardial blood volume (MBV), myocardial blood flow (MBF) and oxygen consumption rate (MVO_2). The biexponential signal (S) originating from a single voxel at a given echo time (TE) can be given by,

$$\frac{S_{voxel}(TE)}{S_0} = e^{-TE/T2_{app}} = MBV \times e^{-TE/T2_b} + (1-MBV) \times e^{-TE/T2_t} \quad (9)$$

where, S_0 is a function of proton density, receiver gain and T1, $T2_{app}$ is the apparent or observed relaxation time while $T2_b$ and $T2_t$ are the T2 values for blood and tissue respectively. $T2_b$ was represented as a parabolic function of oxygen saturation or OEF [23], therefore in the form,

$$\frac{1}{T2_b} = A \times OEF^2 + B \times OEF + C \quad (10)$$

where, A, B and C are relaxation rate constants that were determined using the experimental data of Golay *et al.* [84]. The relaxation within myocardial tissue, $T2_t$ was represented as,

$$\frac{1}{T2_t} = \frac{1}{T2_0} + \frac{1}{T2_{diff}} \quad (11)$$

where, $T2_0$ is the intrinsic myocardial transverse relaxation time and $T2_{diff}$ is the diffusion-sensitive parameter dependent on motion of spins across magnetic field fluctuations in the extravascular space. After simplification, $T2_t$ was rewritten in terms of parameters of interest,

$$\frac{1}{T2_t} = R2_{0t} + R2_{1t} \cdot OEF^2 \cdot MBV^2 \cdot \tau^2 \quad (12)$$

where, $R2_{0t}$ is the reciprocal of $T2_0$ while the second term on the right is the reciprocal of $T2_{diff}$, τ is the interecho spacing. The parameter $R2_{1t}$ is a lumped parameter that represents diffusion constant, susceptibility across the blood-tissue interface, geometry of tissue with respect to field B_0 and size of capillaries. Finally, after appropriate approximations, $OEF_{hyperemia}$ was computed with the equation,

$$\frac{1}{T2_{t,hyperemia}} = R2_{0t} + R2_{1t} \cdot OEF_{hyperemia} \cdot \tau^2 \quad (13)$$

With known OEF_{rest}, $T2_{b,\ rest}$ can be estimated from eqn. 10. Then with known MBV_{rest} and specified TE's, $T2_{t,\ rest}$ can be calculated by fitting the signal in eqn. 9 at multiple TE's. The subject-specific parameters $R2_{0t}$ and $R2_{1t}$ can be estimated by applying two different τ's, computing the corresponding $T2_{t,\ rest}$ using eqn. 9 and then solving the pair of simultaneous equations (eqn. 12), given OEF_{rest} and MBV_{rest}. With system-specific parameters now known, $OEF_{hyperemia}$ can be similarly computed using eqn. 13.

Using the above theoretical basis, Zhang *et al.* [28] assessed the OEF along with myocardial perfusion reserve (MPR) in a canine model of coronary artery stenosis. A turbo spin echo (TSE) in the form of a segmented CPMG acquisition was used with two τ's = 7.3 and 11 ms (3 TE's at each τ). Based on Fick's law, MPR was computed as follows,

$$MPR = \frac{MBF_{hyperemia}}{MBF_{rest}} \approx \frac{OEF_{rest}}{OEF_{hyperemia}} \quad (14)$$

In the myocardium supplied by stenotic artery, T2 demonstrated blunted increase (3%) with vasodilation compared to normal region (10%). The oxygen extraction fraction in affected regions was greater than that in the well-perfused regions (0.43 *vs*. 0.21). The study demonstrated that T2-based BOLD imaging can help distinguish the abnor-

mally perfused territories from normal myocardium in the presence of a defective coronary artery. More recently, McCommis *et al.,* [85] also demonstrated that MRI-based estimation of MBF, OEF and MVO_2 agreed strongly with PET-based measurements (R^2=0.7-0.93), which are considered the gold standard.

FUTURE DIRECTIONS AND CLINICAL APPLICATIONS

The initial *in vitro* studies in blood by Thulborn *et al.,* [20] and Gomori *et al.,* [21] showed that T2 of blood containing deoxygenated hemoglobin increases as the square of the applied magnetic field, suggesting the greater oxygen-sensitivity at higher field strengths. Driven by these observations, the study later by Lee *et al.,* [86] demonstrated the feasibility of using a 3T clinical system to perform *in vivo* oximetric measurements of blood in human femoral vein. In the same study, a 1.5T *vs*. 3T comparison of T2's in blood (*in vitro*) further reinforced that 3T provides greater sensitivity for detecting oxygenation changes (in eqn. 5, $K_{3T}/K_{1.5T}$ = 3.45) with the added advantage of higher signal to noise ratio (SNR), $SNR_{3T}/SNR_{1.5T}$ = 1.35. More recently, Dharmakumar and colleagues [40] have also shown similar benefit of 3T systems over 1.5T with respect to observing BOLD contrast using SSFP-based imaging sequences. A nearly 3-fold increase in oxygen contrast was demonstrated at 3T, compared to 1.5T, in identifying regional perfusion deficits in a canine model of coronary artery stenosis [37].

Based on these initial findings promoting the use higher field strength for increasing the BOLD signal sensitivity, ongoing work in our laboratory has primarily focused on observing the BOLD effect in myocardium at 3T using T2 quantification [87]. We extended the work of Foltz *et al.,* [27] that was performed at 1.5T to a 3T system. Oxygenation changes in the myocardium of healthy (control) pigs were studied in whom stress was induced with Dipyridamole as the vasodilator. As mentioned earlier, Dipyridamole increases blood flow without any significant increase in the cardiac metabolism or myocardial oxygen demand. T2 measurements were then performed on both 1.5T and 3T clinical scanners using a T2-prepared spiral imaging sequence [88] in rest and stress state. Fig. (**6a-e**) shows T2-weighted short-axis slice of representative porcine myocardium imaged at rest on a 3T scanner along with the corresponding T2 map in Fig. (**6f**). As expected T2 values increased with vasodilation as a result of increased blood flow and oxygen saturation, the change thus representing myocardial perfusion reserve. Initial experimental results suggest that a 2-7 fold increase in sensitivity can be obtained at 3T depending on the value of the interecho spacing; theoretical predictions using two-pool model [35] seem to match well with experimental observations.

With respect to potential clinical applications of myocardial BOLD effect, most investigators have focused on identifying regional perfusion deficits in the case of coronary artery stenosis [16,17,19,36,37] with one study looking at hypertensive LV hypertrophy [15]. Our group has recently explored the utility of the T2-based BOLD approach to evaluate regional and longitudinal vasodilatory function in a porcine model of myocardial infarction at 3T [87]. The study involved a 90 min balloon occlusion of the left anterior descending artery (LAD) followed by reperfusion, after which the pigs underwent MRI at 5-6 time points up to 6

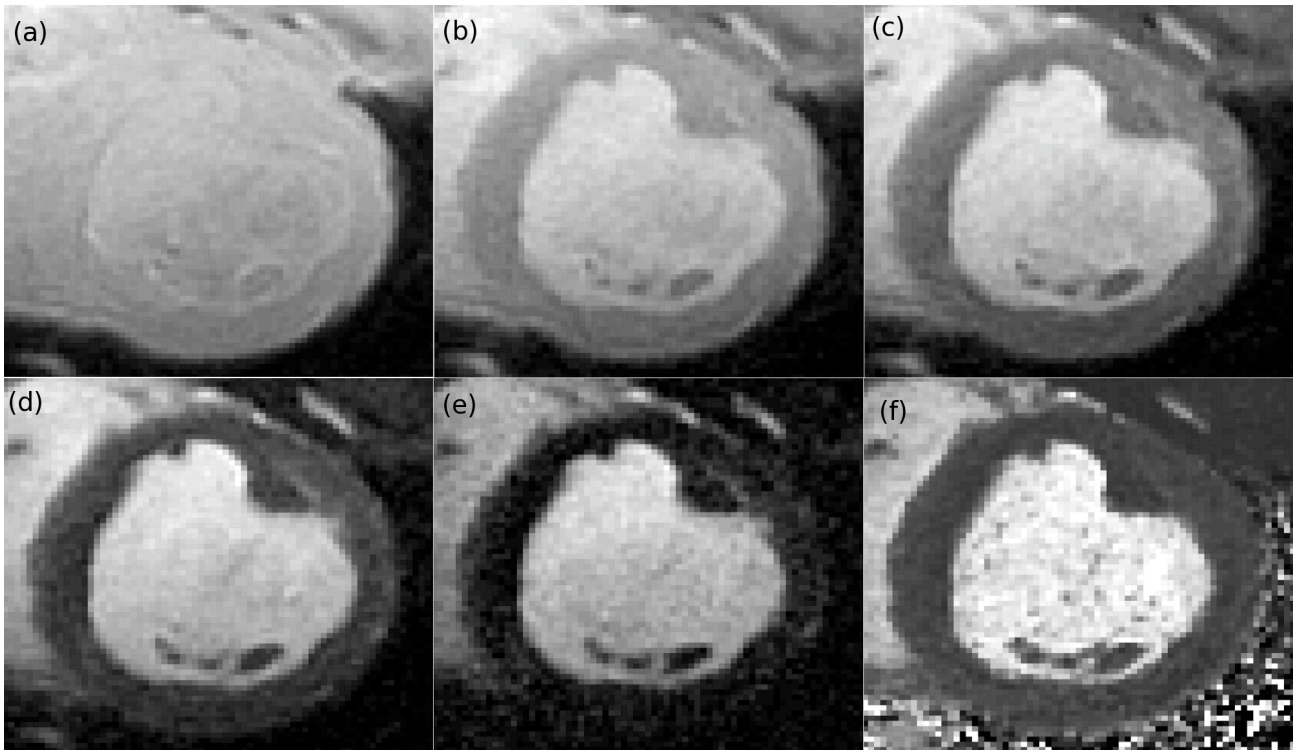

Fig. (6). (**a**) to (**e**) shows images of T2-weighted short axis slice of pig myocardium at rest on a 3T scanner with echo times = 2.9, 24, 48, 88 and 184 ms respectively. (**f**) shows the corresponding pixel-wise computed T2 map with the average T2 value in the anterior region calculated as 41.2 ms.

weeks; control scans were performed before intervention. The infarcted myocardium demonstrated a reduced/null hyperemic response suggesting damaged and/or obstructed microvasculature; a residual response may potentially be indicative of salvageable myocardium in the risk zone. In the remote territories, a subtle increase in resting T2 was observed at week 1-2; this could mean either edema or hyperemia in response to distal infarction. An interesting finding of the study was that the subtle increase in remote T2 was accompanied by a suppressed BOLD-induced stress response that might be indicative of prior vasodilation or a resistive state arising from systemic inflammation or neurohormonal sympathetic activity. These observations were consistent with a previous PET study [89] that demonstrated coronary vasodilator dysfunction in both infarcted and remote myocardium of patients with acute coronary syndrome; despite reperfusion therapy, microvascular integrity and function may be compromised in these territories [89].

Although other imaging strategies such as first-pass perfusion MRI, PET and SPECT and angiographic approaches are routinely used in the clinic to quantify perfusion reserve, BOLD imaging offers the advantage of using endogeneous contrast mechanisms and also being able to provide additional information regarding tissue oxygenation state. This in turn can be translated into the vasodilator function of the microvasculature; for example, vasodilator abnormality in regions supplied by angiographically normal vessels and failure of the vasodilator function to regain control levels at follow-up may potentially be indicative of adverse left ventricular remodeling. Ongoing clinical studies at our institution have demonstrated an elevated resting T2 value in the remote myocardium of patients with large severe infarction (with hemorrhage and microvascular obstruction) [90]. Although no stress test was performed, the observation paralleled that observed in our pig studies; this effect was not observed in patients with smaller non-hemorrhagic infarcts. Similarly, initial studies comparing 45 min and 90 min infarction in pigs have demonstrated that along with infarct zone edema, vasodilator dysfunction in remote myocardium recovers faster in smaller infarcts [91].

Post-infarct remodeling is a complex process and monitoring the evolution of infarcted myocardium is important from a therapeutic perspective [92]. Ultimately, the aim of any therapeutic strategy is to salvage as much myocardium as is possible in the area-at-risk and thereby improve cardiac function and long-term outcomes. Emerging therapeutic pathways/approaches such as reperfusion injury salvage kinase (RISK) pathway, mitochondrial permeability transition pore (PTP), myocardial regeneration using stem cells [93,94] have been successful in animal models however their translation into the clinic has generally been inconclusive. In conjunction with routine clinical protocols, BOLD imaging may potentially offer some new insights into the efficacy of novel therapies and help optimize the timing and duration of their administration.

CONCLUSIONS

Given that the myocardial BOLD effect can be observed using three types of MR imaging sequences – T2*, T2 and SSFP, each has its relative advantage and disadvantage. The T2* technique is quantitative and the most sensitive approach to observe myocardial oxygenation changes, however it is troubled by magnetic susceptibility artifacts arising from the heart-lung interface and deoxygenated blood present in cardiac veins [95]. The SSFP approach is fast, provides high SNR and is advantageous in that it can be used for evaluating cardiac function in addition to providing BOLD contrast. However, being signal intensity-based, it is not quantitative and is limited to resolving regional signal differences within the same subject only. Moreover, it may also be vulnerable to receiver coil-sensitivity issues. Considering these aspects, the T2-based technique may offer a more desirable tool to detect tissue oxygenation changes; it is quantitative, has reasonable SNR and is less prone to magnetic susceptibility artifacts, one disadvantage being the longer acquisition times.

We have reviewed the theoretical formulations and experimental observations made over several years by many investigators who have given significant insight into the oxygen-sensitive nature of T2 relaxation in blood or the T2-based BOLD effect. Early work in blood describing the mechanisms of T2 relaxation as a function of oxygen saturation, field strength and cell integrity paved the way towards *in vivo* determination of tissue oxygenation state. Theoretical modeling in blood and tissue microcirculation further shed light into underlying mechanisms of paramagnetic deoxyhemoglobin, leading the way for interrogating myocardial oxygenation state non invasively. From a clinical standpoint, ongoing pre-clinical studies indicate that quantitative T2 may potentially be more specific than signal intensity measures, allowing regional, longitudinal and cross-subject comparison [87,88]. Lastly, the T2-based BOLD technique offers greater sensitivity on a 3T scanner, compared to 1.5T, allowing reliable detection of serial changes in vasodilator function following acute myocardial infarction.

CONFLICT OF INTEREST

None declared.

ACKNOWLEDGEMENT

None declared.

REFERENCES

[1] Belliveau JW, Kennedy DN Jr., McKinstry RC, *et al*. Functional mapping of the human visual cortex by magnetic resonance imaging. Science 1991; 254(5032): 716-9.

[2] Kwong KK, Belliveau JW, Chesler DA, *et al*. Dynamic magnetic resonance imaging of human brain activity during primary sensory stimulation. Proc Natl Acad Sci USA 1992; 89(12): 5675-9.

[3] Lai S, Hopkins AL, Haacke EM, *et al*. Identification of vascular structures as a major source of signal contrast in high resolution 2D and 3D functional activation imaging of the motor cortex at 1.5T: preliminary results. Magn Reson Med 1993; 30(3): 387-92.

[4] Ogawa S, Lee TM, Nayak AS, Glynn P. Oxygenation-sensitive contrast in magnetic resonance image of rodent brain at high magnetic fields. Magn Reson Med 1990; 14(1): 68-78.

[5] Ogawa S, Menon RS, Tank DW, *et al*. Functional brain mapping by blood oxygenation level-dependent contrast magnetic resonance imaging. A comparison of signal characteristics with a biophysical model. Biophys J 1993; 64(3): 803-12.

[6] Atalay MK, Forder JR, Chacko VP, Kawamoto S, Zerhouni EA. Oxygenation in the rabbit myocardium: assessment with susceptibility-dependent MR imaging. Radiology 1993; 189(3): 759-64.

[7] Balaban RS, Taylor JF, Turner R. Effect of cardiac flow on gradient recalled echo images of the canine heart. NMR Biomed 1994; 7(1-2): 89-95.

[8] Stillman AE, Wilke N, Jerosch-Herold M, *et al*. BOLD contrast of the heart during occlusion and reperfusion. Proc SMR, 1st Annual Meeting: Berkley, Calif 1994: p. S24.

[9] Wendland MF, Saeed M, Lauerma K, de Crespigny A, Moseley ME, Higgins CB. Endogenous susceptibility contrast in myocardium during apnea measured using gradient recalled echo planar imaging. Magn Reson Med 1993; 29(2): 273-6.

[10] Li D, Dhawale P, Rubin PJ, Haacke EM, Gropler RJ. Myocardial signal response to dipyridamole and dobutamine: demonstration of the BOLD effect using a double-echo gradient-echo sequence. Magn Reson Med 1996; 36(1): 16-20.

[11] Niemi P, Poncelet BP, Kwong KK, *et al*. Myocardial intensity changes associated with flow stimulation in blood oxygenation sensitive magnetic resonance imaging. Magn Reson Med 1996; 36(1): 78-82.

[12] Wacker CM, Bock M, Hartlep AW, *et al*. Changes in myocardial oxygenation and perfusion under pharmacological stress with dipyridamole: assessment using T*2 and T1 measurements. Magn Reson Med 1999; 41(4): 686-95.

[13] Bauer WR, Nadler W, Bock M, *et al*. Theory of the BOLD effect in the capillary region: an analytical approach for the determination of T2 in the capillary network of myocardium. Magn Reson Med 1999; 41(1): 51-62.

[14] Bauer WR, Nadler W, Bock M, *et al*. The relationship between the BOLD-induced T(2) and T(2)(*): a theoretical approach for the vasculature of myocardium. Magn Reson Med 1999; 42(6): 1004-10.

[15] Beache GM, Herzka DA, Boxerman JL, *et al*. Attenuated myocardial vasodilator response in patients with hypertensive hypertrophy revealed by oxygenation-dependent magnetic resonance imaging. Circulation 2001; 104(11): 1214-7.

[16] Friedrich MG, Niendorf T, Schulz-Menger J, Gross CM, Dietz R. Blood oxygen level-dependent magnetic resonance imaging in patients with stress-induced angina. Circulation 2003; 108(18): 2219-23.

[17] Wacker CM, Hartlep AW, Pfleger S, Schad LR, Ertl G, Bauer WR. Susceptibility-sensitive magnetic resonance imaging detects human myocardium supplied by a stenotic coronary artery without a contrast agent. J Am Coll Cardiol 2003; 41(5): 834-40.

[18] Egred M, Al-Mohammad A, Waiter GD, *et al*. Detection of scarred and viable myocardium using a new magnetic resonance imaging technique: blood oxygen level dependent (BOLD) MRI. Heart 2003; 89(7): 738-44.

[19] Egred M, Waiter GD, Al-Mohammad A, Semple SI, Redpath TW, Walton S. Blood oxygen level dependent (BOLD) MRI: A novel technique for the detection of myocardial ischemia. Eur J Intern Med 2006; 17(8): 551-5.

[20] Thulborn KR, Waterton JC, Matthews PM, Radda GK. Oxygenation dependence of the transverse relaxation time of water protons in whole blood at high field. Biochim Biophys Acta 1982; 714(2): 265-70.

[21] Gomori JM, Grossman RI, Yu-Ip C, Asakura T. NMR relaxation times of blood: dependence on field strength, oxidation state, and cell integrity. J Comput Assist Tomogr 1987; 11(4): 684-90.

[22] Meyer ME, Yu O, Eclancher B, Grucker D, Chambron J. NMR relaxation rates and blood oxygenation level. Magn Reson Med 1995; 34(2): 234-41.

[23] Wright GA, Hu BS, Macovski A. 1991 I.I. Rabi Award. Estimating oxygen saturation of blood *in vivo* with MR imaging at 1.5 T. J Magn Reson Imaging 1991; 1(3): 275-83.

[24] Foltz WD, Merchant N, Downar E, Stainsby JA, Wright GA. Coronary venous oximetry using MRI. Magn Reson Med 1999; 42(5): 837-48.

[25] Yang Y, Foltz WD, Merchant N, Stainsby JA, Wright GA. Noninvasive quantitative measurement of myocardial and whole-body oxygen consumption using MRI: initial results. Magn Reson Imaging 2009; 27(2): 147-54.

[26] Atalay MK, Reeder SB, Zerhouni EA, Forder JR. Blood oxygenation dependence of T1 and T2 in the isolated, perfused rabbit heart at 4.7T. Magn Reson Med 1995; 34(4): 623-7.

[27] Foltz WD, Huang H, Fort S, Wright GA. Vasodilator response assessment in porcine myocardium with magnetic resonance relaxometry. Circulation 2002; 106(21): 2714-9.

[28] Zhang H, Gropler RJ, Li D, Zheng J. Assessment of myocardial oxygen extraction fraction and perfusion reserve with BOLD imaging in a canine model with coronary artery stenosis. J Magn Reson Imaging 2007; 26(1): 72-9.

[29] Zheng J, Wang J, Nolte M, Li D, Gropler RJ, Woodard PK. Dynamic estimation of the myocardial oxygen extraction ratio during dipyridamole stress by MRI: a preliminary study in canines. Magn Reson Med 2004; 51(4): 718-26.

[30] Zheng J, Wang J, Rowold FE, Gropler RJ, Woodard PK. Relationship of apparent myocardial T2 and oxygenation: towards quantification of myocardial oxygen extraction fraction. J Magn Reson Imaging 2004; 20(2): 233-41.

[31] Fieno DS, Shea SM, Li Y, Harris KR, Finn JP, Li D. Myocardial perfusion imaging based on the blood oxygen level-dependent effect using T2-prepared steady-state free-precession magnetic resonance imaging. Circulation 2004; 110(10): 1284-90.

[32] Shea SM, Fieno DS, Schirf BE, *et al*. T2-prepared steady-state free precession blood oxygen level-dependent MR imaging of myocardial perfusion in a dog stenosis model. Radiology 2005; 236(2): 503-9.

[33] Wright KB, Klocke FJ, Deshpande VS, *et al*. Assessment of regional differences in myocardial blood flow using T2-weighted 3D BOLD imaging. Magn Reson Med 2001; 46(3): 573-8.

[34] Noseworthy MD, Kim JK, Stainsby JA, Stanisz GJ, Wright GA. Tracking oxygen effects on MR signal in blood and skeletal muscle during hyperoxia exposure. J Magn Reson Imaging 1999; 9(6): 814-20.

[35] Stainsby JA, Wright GA. Monitoring blood oxygen state in muscle microcirculation with transverse relaxation. Magn Reson Med 2001; 45(4): 662-72.

[36] Dharmakumar R, Arumana JM, Larson AC, Chung Y, Wright GA, Li D. Cardiac phase-resolved blood oxygen-sensitive steady-state free precession MRI for evaluating the functional significance of coronary artery stenosis. Invest Radiol 2007; 42(3): 180-8.

[37] Dharmakumar R, Arumana JM, Tang R, Harris K, Zhang Z, Li D. Assessment of regional myocardial oxygenation changes in the presence of coronary artery stenosis with balanced SSFP imaging at 3.0 T: theory and experimental evaluation in canines. J Magn Reson Imaging 2008; 27(5): 1037-45.

[38] Dharmakumar R, Hong J, Brittain JH, Plewes DB, Wright GA. Oxygen-sensitive contrast in blood for steady-state free precession imaging. Magn Reson Med 2005; 53(3): 574-83.

[39] Luz Z, Meiboom S. Nuclear magnetic resonance study of the protolysis of trimethylammonium iron in aqueous solution: order of the reaction with respect to the solvent. J Chem Phys 1963; 39: 366-70.

[40] Dharmakumar R, Qi X, Hong J, Wright GA. Detecting microcirculatory changes in blood oxygen state with steady-state free precession imaging. Magn Reson Med 2006; 55(6): 1372-80.

[41] Arumana JM, Li D, Dharmakumar R. Deriving blood-oxygen-level-dependent contrast in MRI with T2*-weighted, T2-prepared and phase-cycled SSFP methods: theory and experiment. Magn Reson Med 2008; 59(3): 561-70.

[42] Klarhofer M, Madorin P, Bilecen D, Scheffler K. Assessment of muscle oxygenation with balanced SSFP: a quantitative signal analysis. J Magn Reson Imaging 2008; 27(5): 1169-74.

[43] Scheffler K, Seifritz E, Bilecen D, *et al*. Detection of BOLD changes by means of a frequency-sensitive trueFISP technique: preliminary results. NMR Biomed 2001; 14(7-8): 490-6.

[44] Pauling L. Magnetic properties and structure of oxyhemoglobin. Proc Natl Acad Sci USA 1977; 74(7): 2612-3.

[45] Pauling L, Coryell CD. The Magnetic Properties and Structure of Hemoglobin, Oxyhemoglobin and Carbonmonoxyhemoglobin. Proc Natl Acad Sci USA 1936; 22(4): 210-6.

[46] Pauling L, Coryell CD. The Magnetic Properties and Structure of the Hemochromogens and Related Substances. Proc Natl Acad Sci USA 1936; 22(3): 159-63.

[47] Bloembergen N, Purcell EM, Pound RV. Relaxation effects in nuclear magnetic resonance absorbtion. Phys Rev 1948; 73: 679.

[48] Allerhand A, Gutowsky HS. Spin-echo NMR studies of chemical exchange. I. Some general aspects. J Chem Phys 1964; 41: 2115.

[49] Brooks RA, Di Chiro G. Magnetic resonance imaging of stationary blood: a review. Med Phys 1987; 14(6): 903-13.

[50] Hayman LA, Ford JJ, Taber KH, Saleem A, Round ME, Bryan RN. T2 effect of hemoglobin concentration: assessment with *in vitro* MR spectroscopy. Radiology 1988; 168(2): 489-91.

[51] Terrier F, Lazeyras F, Posse S, *et al*. Study of acute renal ischemia in the rat using magnetic resonance imaging and spectroscopy. Magn Reson Med 1989; 12(1): 114-36.

[52] Brooks RA, Brunetti A, Alger JR, Di Chiro G. On the origin of paramagnetic inhomogeneity effects in blood. Magn Reson Med 1989; 12(2): 241-8.

[53] Gillis P, Koenig SH. Transverse relaxation of solvent protons induced by magnetized spheres: application to ferritin, erythrocytes, and magnetite. Magn Reson Med 1987; 5(4): 323-45.

[54] Matwiyoff NA, Gasparovic C, Mazurchuk R, Matwiyoff G. The line shapes of the water proton resonances of red blood cells containing carbonyl hemoglobin, deoxyhemoglobin, and methemoglobin: implications for the interpretation of proton MRI at fields of 1.5 T and below. Magn Reson Imaging 1990; 8(3): 295-301.

[55] Bryant RG, Marill K, Blackmore C, Francis C. Magnetic relaxation in blood and blood clots. Magn Reson Med 1990; 13(1): 133-44.

[56] Levitt M, Freeman R, Frenkiel T. Broadband decoupling in high-resolution nuclear magnetic resonance spectroscopy. Adv Magn Reson 1983; 11: 47-108.

[57] Wilson RF, Johnson MR, Marcus ML, *et al*. The effect of coronary angioplasty on coronary flow reserve. Circulation 1988; 77(4): 873-85.

[58] Wilson RF, White CW. Does coronary artery bypass surgery restore normal maximal coronary flow reserve? The effect of diffuse atherosclerosis and focal obstructive lesions. Circulation 1987; 76(3): 563-71.

[59] Marchant E, Pichard A, Rodriguez JA, Casanegra P. Acute effect of systemic versus intracoronary dipyridamole on coronary circulation. Am J Cardiol 1986; 57(15): 1401-4.

[60] Hundley WG, Lange RA, Clarke GD, *et al*. Assessment of coronary arterial flow and flow reserve in humans with magnetic resonance imaging. Circulation 1996; 93(8): 1502-8.

[61] Li KC, Dalman RL, Ch'en IY, *et al*. Chronic mesenteric ischemia: use of *in vivo* MR imaging measurements of blood oxygen saturation in the superior mesenteric vein for diagnosis. Radiology 1997; 204(1): 71-7.

[62] Li KC, Pelc LR, Dalman RL, *et al*. *In vivo* magnetic resonance evaluation of blood oxygen saturation in the superior mesenteric vein as a measure of the degree of acute flow reduction in the superior mesenteric artery: findings in a canine model. Acad Radiol 1997; 4(1): 21-5.

[63] Li KC, Wright GA, Pelc LR, *et al*. Oxygen saturation of blood in the superior mesenteric vein: *in vivo* verification of MR imaging measurements in a canine model. Work in progress. Radiology 1995; 194(2): 321-5.

[64] Nield LE, Qi X, Yoo SJ, Valsangiacomo ER, Hornberger LK, Wright GA. MRI-based blood oxygen saturation measurements in infants and children with congenital heart disease. Pediatr Radiol 2002; 32(7): 518-22.

[65] Nield LE, Qi XL, Valsangiacomo ER, *et al*. *In vivo* MRI measurement of blood oxygen saturation in children with congenital heart disease. Pediatr Radiol 2005; 35(2): 179-85.

[66] Bengel FM, Permanetter B, Ungerer M, Nekolla S, Schwaiger M. Non-invasive estimation of myocardial efficiency using positron emission tomography and carbon-11 acetate--comparison between the normal and failing human heart. Eur J Nucl Med 2000; 27(3): 319-26.

[67] Arena R, Myers J, Aslam SS, Varughese EB, Peberdy MA. Peak VO2 and VE/VCO2 slope in patients with heart failure: a prognostic comparison. Am Heart J 2004; 147(2): 354-60.

[68] Kavanagh T, Mertens DJ, Hamm LF, *et al*. Prediction of long-term prognosis in 12 169 men referred for cardiac rehabilitation. Circulation 2002; 106(6): 666-71.

[69] Iida H, Rhodes CG, Araujo LI, *et al*. Noninvasive quantification of regional myocardial metabolic rate for oxygen by use of 15O2 inhalation and positron emission tomography. Theory, error analysis, and application in humans. Circulation 1996; 94(4): 792-807.

[70] Frewen TC, Sumabat WO, Del Maestro RF. Cerebral blood flow, metabolic rate, and cross-brain oxygen consumption in brain injury. J Pediatr 1985; 107(4): 510-3.

[71] Klintmalm GB, Cronestrand R, Wennmalm A, Lundgren G, Groth CG. Human renal allograft blood flow, oxygen extraction, and prostaglandin release: their bearing on graft function. Surgery 1984; 95(4): 427-32.

[72] Mezey E. Commentary on the hypermetabolic state and the role of oxygen in alcohol-induced liver injury. Recent Dev Alcohol 1984; 2: 135-41.

[73] Tran TK, Sailasuta N, Hurd R, Jue T. Spatial distribution of deoxymyoglobin in human muscle: an index of local tissue oxygenation. NMR Biomed 1999; 12(1): 26-30.

[74] Wariar R, Gaffke JN, Haller RG, Bertocci LA. A modular NIRS system for clinical measurement of impaired skeletal muscle oxygenation. J Appl Physiol 2000; 88(1): 315-25.

[75] Adzamli IK, Jolesz FA, Bleier AR, Mulkern RV, Sandor T. The effect of gadolinium DTPA on tissue water compartments in slow- and fast-twitch rabbit muscles. Magn Reson Med 1989; 11(2): 172-81.

[76] Belton PS, Jackson RR, Packer KJ. Pulsed NMR studies of water in striated muscle. I. Transverse nuclear spin relaxation times and freezing effects. Biochim Biophys Acta 1972; 286(1): 16-25.

[77] English AE, Joy ML, Henkelman RM. Pulsed NMR relaxometry of striated muscle fibers. Magn Reson Med 1991; 21(2): 264-81.

[78] Hazlewood CF, Chang DC, Nichols BL, Woessner DE. Nuclear magnetic resonance transverse relaxation times of water protons in skeletal muscle. Biophys J 1974; 14(8): 583-606.

[79] Le Rumeur E, De Certaines J, Toulouse P, Rochcongar P. Water phases in rat striated muscles as determined by T2 proton NMR relaxation times. Magn Reson Imaging 1987; 5(4): 267-72.

[80] Donahue KM, Weisskoff RM, Chesler DA, *et al*. Improving MR quantification of regional blood volume with intravascular T1 contrast agents: accuracy, precision, and water exchange. Magn Reson Med 1996; 36(6): 858-67.

[81] Fabry ME, Eisenstadt M. Water exchange across red cell membranes: II. Measurements by nuclear magnetic resonance T1, T2, and T12 hybrid relaxation. The effects of osmolarity, cell volume, and medium. J Membr Biol 1978; 42(4): 375-98.

[82] Bauer WR, Hiller KH, Roder F, Rommel E, Ertl G, Haase A. Magnetization exchange in capillaries by microcirculation affects diffusion-controlled spin-relaxation: a model which describes the effect of perfusion on relaxation enhancement by intravascular contrast agents. Magn Reson Med 1996; 35(1): 43-55.

[83] Klocke FJ, Simonetti OP, Judd RM, *et al*. Limits of detection of regional differences in vasodilated flow in viable myocardium by first-pass magnetic resonance perfusion imaging. Circulation 2001; 104(20): 2412-6.

[84] Golay X, Silvennoinen MJ, Zhou J, *et al*. Measurement of tissue oxygen extraction ratios from venous blood T(2): increased precision and validation of principle. Magn Reson Med 2001; 46(2): 282-91.

[85] McCommis KS, Zhang H, Herrero P, Gropler RJ, Zheng J. Feasibility study of myocardial perfusion and oxygenation by noncontrast MRI: comparison with PET study in a canine model. Magn Reson Imaging 2008; 26(1): 11-9.

[86] Lee T, Stainsby JA, Hong J, Han E, Brittain JH, Wright GA. Blood relaxation properties at 3T -- Effects of blood oxygen saturation. 2003; Proc Intl Soc Mag Reson Med, 11th Annual Meeting. Toronto 2003; p. 131.

[87] Ghugre NR, Ramanan V, Pop M, *et al*. Myocardial BOLD imaging at 3 T using quantitative T(2) : Application in a myocardial infarct model. Magn Reson Med 2011; 66(6): 1739-47.

[88] Ghugre NR, Ramanan V, Pop M, *et al*. Quantitative tracking of edema, hemorrhage, and microvascular obstruction in subacute myocardial infarction in a porcine model by MRI. Magn Reson Med 2011; 66(4): 1129-41.

[89] Uren NG, Crake T, Lefroy DC, de Silva R, Davies GJ, Maseri A. Reduced coronary vasodilator function in infarcted and normal

myocardium after myocardial infarction. N Engl J Med 1994; 331(4): 222-7.

[90] Zia M, Ghugre N, Paul G, *et al*. Characterizing myocardial edema and hemorrhage using T2, T2*, and diastolic wall thickness post acute myocardial infarction. J Cardiov Magn Reson 2010; 12(Suppl 1): P179.

[91] Ghugre N, Barry J, Qiang B, *et al*. Longitudinal trends of remodeling mechanisms after acute myocardial infarction based on severity of ischemic insult: A quantitative MRI study. J Cardiov Magn Reson 2011; 13(Suppl 1): O57.

[92] Jugdutt BI. Ventricular remodeling after infarction and the extracellular collagen matrix: when is enough enough? Circulation 2003; 108(11): 1395-403.

[93] Yellon DM, Hausenloy DJ. Myocardial reperfusion injury. N Engl J Med 2007; 357(11): 1121-35.

[94] Orlic D, Hill JM, Arai AE. Stem cells for myocardial regeneration. Circ Res 2002; 91(12): 1092-102.

[95] Reeder SB, Faranesh AZ, Boxerman JL, McVeigh ER. *In vivo* measurement of T*2 and field inhomogeneity maps in the human heart at 1.5 T. Magn Reson Med 1998; 39(6): 988-98.

Received: December 29, 2010 Revised: December 22, 2011 Accepted: December 22, 2011

© Ghugre and Wright; Licensee *Bentham Open*.

This is an open access article licensed under the terms of the Creative Commons Attribution Non-Commercial License (http://creativecommons.org/licenses/by-nc/3.0/), which permits unrestricted, non-commercial use, distribution and reproduction in any medium, provided the work is properly cited.